Multipass laser cavity for efficient transverse illumination of an elongated volume

Jan Vogelsang,[1] Marc Diepold,[1] Aldo Antognini,[2] Andreas Dax,[3] Johannes Götzfried,[1] Theodor W. Hänsch,[1] Franz Kottmann,[2] Julian J. Krauth,[1] Yi-Wei Liu,[4] Tobias Nebel,[1] Francois Nez,[5] Karsten Schuhmann,[2,3] David Taqqu,[3] and Randolf Pohl[1,*]

[1]*Max–Planck–Institut für Quantenoptik, 85748 Garching, Germany*
[2]*Institute for Particle Physics, ETH Zurich, 8093 Zurich, Switzerland*
[3]*Paul Scherrer Institute, 5232 Villigen–PSI, Switzerland*
[4]*Physics Department, National Tsing Hua University, Hsinchu 300, Taiwan*
[5]*Laboratoire Kastler Brossel, École Normale Supérieure, CNRS and Université P. et M. Curie, 75252 Paris, CEDEX 05, France*
[*]*randolf.pohl@mpq.mpg.de*

Abstract: A multipass laser cavity is presented which can be used to illuminate an elongated volume from a transverse direction. The illuminated volume can also have a very large transverse cross section. Convenient access to the illuminated volume is granted. The multipass cavity is very robust against misalignment, and no active stabilization is needed. The scheme is suitable for example in beam experiments, where the beam path must not be blocked by a laser mirror, or if the illuminated volume must be very large. This cavity was used for the muonic-hydrogen experiment in which 6 μm laser light illuminated a volume of $7 \times 25 \times 176\,\mathrm{mm}^3$, using mirrors that are only 12 mm in height. We present our measurement of the intensity distribution inside the multipass cavity and show that this is in good agreement with our simulation.

OCIS codes: (080.4035) Mirror system design.

References and links

1. R. Pohl, A. Antognini, F. Nez, F. D. Amaro, F. Biraben, J. M. R. Cardoso, D. S. Covita, A. Dax, S. Dhawan, L. M. P. Fernandes, A. Giesen, T. Graf, T. W. Hänsch, P. Indelicato, L. Julien, C.-Y. Kao, P. Knowles, E.-O. L. Bigot, Y.-W. Liu, J. A. M. Lopes, L. Ludhova, C. M. B. Monteiro, F. Mulhauser, T. Nebel, P. Rabinowitz, J. M. F. dos Santos, L. A. Schaller, K. Schuhmann, C. Schwob, D. Taqqu, J. F. C. A. Veloso, and F. Kottmann, "The size of the proton," Nature **466**, 213 (2010).
2. A. Antognini, F. Nez, K. Schuhmann, F. D. Amaro, F. Biraben, J. M. R. Cardoso, D. S. Covita, A. Dax, S. Dhawan, M. Diepold, L. M. P. Fernandes, A. Giesen, T. Graf, A. L. Gouvea, T. W. Hänsch, P. Indelicato, L. Julien, C.-Y. Kao, P. Knowles, F. Kottmann, E.-O. L. Bigot, Y.-W. Liu, J. A. M. Lopes, L. Ludhova, C. M. B. Monteiro, F. Mulhauser, T. Nebel, P. Rabinowitz, J. M. F. dos Santos, L. A. Schaller, C. Schwob, D. Taqqu, J. F. C. A. Veloso, J. Vogelsang, and R. Pohl, "Proton structure from the measurement of 2S-2P transition frequencies of muonic hydrogen," Science **339**, 417 (2013).
3. R. Pohl, H. Daniel, F. J. Hartmann, P. Hauser, F. Kottmann, V. E. Markushin, M. Muhlbauer, C. Petitjean, W. Schott, D. Taqqu, and P. Wojciechowski-Grosshauser, "Observation of long-lived muonic hydrogen in the 2S state," Phys. Rev. Lett. **97**, 193402 (2006).
4. L. Fernandes, A. Antognini, M. Boucher, C. Conde, O. Huot, P. Knowles, F. Kottmann, L. Ludhova, F. Mulhauser, R. Pohl, L. Schaller, J. dos Santos, D. Taqqu, and J. Veloso, "Behaviour of large-area avalanche photodiodes under intense magnetic fields for vuv-, visible-, and x-ray photon detection," Nucl. Inst. Meth. A **498**, 362–368 (2003).

#206146 - $15.00 USD Received 11 Feb 2014; revised 22 Apr 2014; accepted 23 Apr 2014; published 22 May 2014

5. L. Ludhova, F. D. Amaro, A. Antognini, F. Biraben, J. M. R. Cardoso, C. A. N. Conde, D. S. Covita, A. Dax, S. Dhawan, L. M. P. Fernandes, T. W. Hänsch, V.-W. Hughes, O. Huot, P. Indelicato, L. Julien, P. E. Knowles, F. Kottmann, J. A. M. Lopes, Y.-W. Liu, C. M. B. Monteiro, F. Mulhauser, F. Nez, R. Pohl, P. Rabinowitz, J. M. F. dos Santos, L. A. Schaller, D. Taqqu, and J. F. C. A. Veloso, "Planar LAAPDs: temperature dependence, performance, and application in low-energy x-ray spectroscopy," Nucl. Inst. Meth. A **540**, 169–179 (2005).
6. A. Antognini, F. D. Amaro, F. Biraben, J. M. R. Cardoso, C. A. N. Conde, D. S. Covita, A. Dax, S. Dhawan, L. M. P. Fernandes, T. W. Hänsch, V. . Hughes, O. Huot, P. Indelicato, L. Julien, P. E. Knowles, F. Kottmann, Y.-W. Liu, J. A. M. Lopes, L. Ludhova, C. M. B. Monteiro, F. Mulhauser, F. Nez, B. N. Perry, R. Pohl, P. Rabinowitz, J. M. F. dos Santos, L. A. Schaller, C. Schwob, D. Taqqu, and J. F. C. A. Veloso, "Powerful fast triggerable 6 μm laser for the muonic hydrogen 2S-Lamb shift experiment," Opt. Comm. **253**, 362–374 (2005).
7. A. Antognini, K. Schuhmann, F. D. Amaro, F. Biraben, A. Dax, A. Giesen, T. Graf, T. W. Hänsch, P. Indelicato, L. Julien, K. Cheng-Yang, P. E. Knowles, F. Kottmann, E. Le Bigot, Y.-W. Liu, L. Ludhova, N. Moschüring, F. Mulhauser, T. Nebel, F. Nez, P. Rabinowitz, C. Schwob, D. Taqqu, and R. Pohl, "Thin-disk Yb:YAG oscillator-amplifier laser, ASE, and effective Yb:YAG lifetime," IEEE J. Quant. Electr. **45**, 993–1005 (2009).
8. A. Antognini, F. Nez, F. D. Amaro, F. Biraben, J. M. R. Cardoso, D. S. Covita, A. Dax, S. Dhawan, L. M. P. Fernandes, A. Giesen, T. Graf, T. W. Hänsch, P. Indelicato, L. Julien, C.-Y. Kao, P. Knowles, F. Kottmann, E.-O. L. Bigot, Y.-W. Liu, J. A. M. Lopes, L. Ludhova, C. M. B. Monteiro, F. Mulhauser, T. Nebel, P. Rabinowitz, J. M. F. dos Santos, L. A. Schaller, K. Schuhmann, C. Schwob, D. Taqqu, J. F. C. A. Veloso, and R. Pohl, "Illuminating the proton radius conundrum: the μHe$^+$ Lamb shift," Can. J. Phys. **89**, 47 (2010).
9. Dama technologies ag, Romanshornerstrasse 7, 9308 Lömmenschwil, Switzerland.
10. S. Romanov, "On the photoexcitation of the 2s→2p transition in light muonic atoms," Z. Phys. D **33**, 17–26 (1995).
11. Lens-Optics GmbH, Bürgermeister-Neumeyr-Strasse 7, 85391 Allershausen, Germany.
12. Agilent Technologies, 5301 Stevens Creek Boulevard, Santa Clara, CA 95051, USA.
13. Epoxy Technology, 14 Fortune Drive, Billerica, MA 01821, USA.
14. Umicore Coating Services Ltd., Kinnoull St, Dundee, Dundee City DD2 3ED, UK.
15. LohnStar Optics, 1863 Commercial St., Escondido, CA 92029, USA.
16. Advanced Thin Films, 5733 Central Ave., Boulder, CO 80301, USA.
17. J. L. Flowers, P. E. G. Baird, L. Bougueroua, H. A. Klein, and H. S. Margolis, "The NPL Rydberg constant experiment." IEEE Trans. Instrum. Meas. **56**, 331–335 (2007).
18. A. Beyer, J. Alnis, K. Khabarova, A. Matveev, C. G. Parthey, D. C. Yost, R. Pohl, Th. Udem, T. W. Hänsch, and N. Kolachevsky, "Precision spectroscopy of the 2s-4p transition in atomic hydrogen on a cryogenic beam of optically excited 2S atoms," Ann. d. Phys. (Berlin) **525**, 671 (2013).
19. N. Kuroda, S. Ulmer, D. J. Murtagh, S. V. Gorp, Y. Nagata, M. Diermaier, S. Federmann, M. Leali, C. Malbrunot, V. Mascagna, O. Massiczek, K. Michishio, T. Mizutani, A. Mohri, H. Nagahama, M. Ohtsuka, B. Radics, S. Sakurai, C. Sauerzopf, K. Suzuki, M. Tajima, H. A. Torii, L. Venturelli, B. Wünschek, J. Zmeskal, N. Zurlo, H. Higaki, Y. Kanai, E. L. Rizzini, Y. Nagashima, Y. Matsuda, E. Widmann, and Y. Yamazaki, "A source of antihydrogen for in-flight hyperfine spectroscopy," Nature Comm. **5**, 3089 (2013).
20. R. Ferragut, A. S. Belov, G. Bonomi, I. Boscolo, R. S. Brusa, V. Byakov, L. Cabaret, A. Calloni, C. Canali, C. Carraro, F. Castelli, S. Cialdi, D. Comparat, G. Consolati, L. Dassa, N. Djourelov, M. Doser, G. Drobychev, A. Dudarev, A. Dupasquier, G. Ferrari, A. Fischer, P. Folegati, A. Fontana, L. Formaro, M. G. Giammarchi, S. N. Gninenko, R. Heyne, S. D. Hogan, L. V. Jorgensen, A. Kellerbauer, D. Krasnicky, V. Lagomarsino, G. Manuzio, S. Mariazzi, V. A. Matveev, C. Morhard, G. Nebbia, P. Nedelec, M. K. Oberthaler, D. Perini, V. Petracek, F. Prelz, M. Prevedelli, I. Y. Al-Qaradawi, F. Quasso, C. Riccardi, O. Rohne, A. Rotondi, M. Sacerdoti, H. Sandaker, D. Sillou, S. V. Stepanov, H. H. Stroke, G. Testera, D. Trezzi, A. V. Turbabin, R. Vaccarone, F. Villa, U. Warring, S. Zavatarelli, A. Zenoni, , and D. Zvezhinskij, "Antihydrogen physics: gravitation and spectroscopy in AEgIS," Can. J. Phys. **89**, 17–24 (2011).
21. G. Chardin, P. Grandemange, D. Lunney, V. Manea, A. Badertscher, P. Crivelli, A. Curioni, A. Marchionni, B. Rossi, A. Rubbia, V. Nesvizhevsky, P. Hervieux, G. Manfredi, P. Comini, P. Debu, P. Dupré, L. Liszkay, B. Mansoulié, P. Pérez, J. Rey, N. Ruiz, Y. Sacquin, A. Voronin, F. Biraben, P. Cladé, A. Douillet, A. Gérardin, S. Guellati, L. Hilico, P. Indelicato, A. Lambrecht, R. Guérout, J. Karr, F. Nez, S. Reynaud, V. Tran, A. Mohri, Y. Yamazaki, M. Charlton, S. Eriksson, N. Madsen, D. van der Werf, N. Kuroda, H. Torii, and Y. Nagashima, "Proposal to measure the gravitational behaviour of antihydrogen at rest," Tech. Rep. CERN-SPSC-2011-029.SPSC-P-342, CERN, Geneva (2011).
22. C. Amole, M. D. Ashkezari, M. Baquero-Ruiz, W. Bertsche, E. Butler, A. Capra, C. L. Cesar, M. Charlton, S. Eriksson, J. Fajans, T. Friesen, M. C. Fujiwara, D. R. Gill, A. Gutierrez, J. S. Hangst, W. N. Hardy, M. E. Hayden, C. A. Isaac, S. Jonsell, L. Kurchaninov, A. Little, N. Madsen, J. T. K. McKenna, S. Menary, S. C. Napoli, P. Nolan, A. Olin, P. Pusa, C. O. Rasmussen, F. Robicheaux, E. Sarid, D. M. Silveira, C. So, R. I. Thompson, D. P. van der Werf, J. S. Wurtele, A. I. Zhmoginov, and A. E. Charman, "Description and first application of a new technique to measure the gravitational mass of antihydrogen," Nature Comm. **4**, 1785 (2013).
23. This particular geometry requires 220 mm long and 15 mm high mirrors, separated by 100 mm. The cylinder mirror can have a radius of curvature of R = 500 mm, and the cylindircal end pieces have R = 200 mm.

#206146 - $15.00 USD Received 11 Feb 2014; revised 22 Apr 2014; accepted 23 Apr 2014; published 22 May 2014

24. A. Antognini, P. Crivelli, T. Prokscha, K. S. Khaw, B. Barbiellini, L. Liszkay, K. Kirch, K. Kwuida, E. Morenzoni, F. M. Piegsa, Z. Salman, and A. Suter, "Muonium emission into vacuum from mesoporous thin films at cryogenic temperatures," Phys. Rev. Lett. **108**, 143401 (2012).
25. J. Allen P. Mills, "Precision experiments with ultraslow muons," JPS Conf. Proc. **2**, 010401 (2014). Proc. Int. Symp. Science Explored by Ultra Slow Muon (USM2013).
26. P. Crivelli, C. L. Cesar, and U. Gendotti, "Advances towards a new measurement of the 1S–2S transition of positronium," Can. J. Phys. **89**, 29 (2010).
27. D. B. Cassidy, T. H. Hisakado, H. W. K. Tom, and A. P. Mills, "Efficient production of Rydberg Positronium," Phys. Rev. Lett. **108**, 043401 (2012).
28. W. Schott, T. Faestermann, P. Fierlinger, F. J. Hartmann, R. Hertenberger, A. R. Müller, S. Paul, J. Schön, Th. Udem, and A. Ulrich, "An experiment to measure the bound-β-decay of the free neutron," Hyp. Interact. **193**, 269 (2009).

1. Introduction

Experiments with particle beams at times require illumination of an elongated volume, i.e. over a length which is much larger than the transverse dimension of the beam. One solution would be to intersect a laser beam at some finite angle with respect to the particle beam such that the particle beam is not obscured by laser mirrors. This usually results in a poor overlap between the particle beam and the laser beam.

In addition, such an arrangement allows only illumination of a volume with small transverse dimensions if a cavity is used to increase the laser fluence. Cavities with larger beam waists would require cavity mirrors with exceedingly large radii of curvature, which makes such a cavity unstable.

Here we present a multipass mirror cavity that can be used to efficiently illuminate, from the transverse direction, a volume with a length of several tens of cm or more, limited only by the mirror reflectivity. In addition, the illuminated volume can have a large transverse size. The beam volume is not obscured by the mirrors, allowing for large-solid-angle detection of photons. In addition, the mirror cavity is extremely robust against misalignments making control and stabilization of the mirrors unnecessary.

The mirror cavity shown in Fig. 1 was used to illuminate the 200 mm long stop volume of

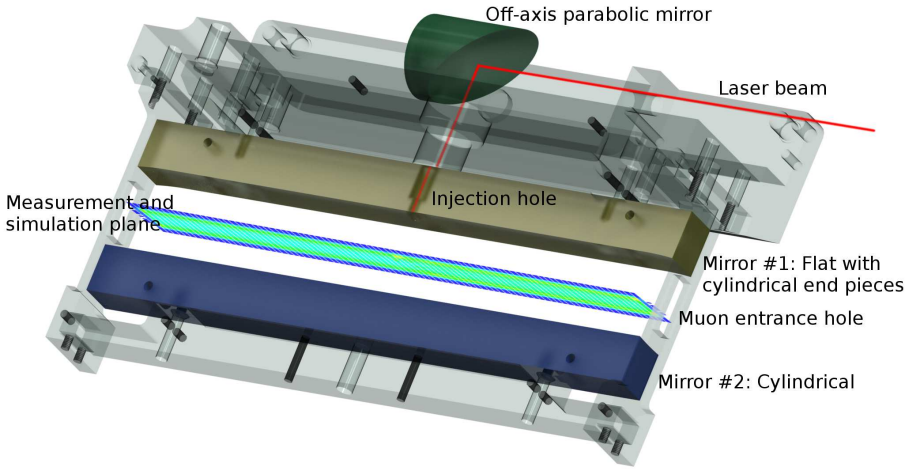

Fig. 1. Complete setup of the multipass laser cavity, with mounts and injection optics. Also indicated is the cavity mid-plane where the intensity distribution is measured and simulated.

#206146 - $15.00 USD Received 11 Feb 2014; revised 22 Apr 2014; accepted 23 Apr 2014; published 22 May 2014

muons injected into low pressure H_2 gas. The setup was used for the recent determination of the proton charge radius via laser spectroscopy of the exotic muonic hydrogen atom [1, 2]. The low gas pressure of only 1 mbar (at room temperature) is necessary to avoid collisional processes which shorten the lifetime of the muonic hydrogen atoms [3]. The low gas density results in an approximately pencil-sized stop volume with a length of 200 mm. The transverse dimension of the muon stop volume to be illuminated is 12 mm (width) times 5 mm (height). Several large-area avalanche photo diodes [4, 5] ($14 \times 14\,\mathrm{mm}^2$ active surface) were placed as close as 8 mm from the muon beam axis to maximize the solid angle for the detection of x-rays from muonic hydrogen.

Each incoming muon triggers a pulsed laser system [6, 7], tunable around $\lambda \approx 6\,\mu$m. We obtained pulses of 0.25 mJ energy, with a pulse length of 5 ns. The multipass mirror cavity described in here was used to illuminate the elongated muon stop volume from the transverse direction. We realized a rather homogeneous ($\pm 30\%$) illumination of the stop volume and confined the laser pulse for approximately 55 ns, corresponding to about 670 reflections of the light inside the cavity, limited by the reflectivity of the coating of $R \approx 99.89\,\%$.

The cavity is installed inside a superconducting 5 Tesla solenoid which is then evacuated. Our cavity design proved to be very robust against misalignments, and no active stabilization was required over weeks of continuous data taking.

Three different cavities have been built with their main difference being the high reflective (HR) coating (see Sec. 6.3):

- Cavity A had a ThF_4 / ZnSe HR coating optimized for $\lambda \in [5.5 \ldots 6.1]\,\mu$m, but displayed a reflectivity better than 99.9 % around 850 nm. This cavity was used in a test setup to produce most of the plots shown here, using a laser diode at 850 nm.

- Cavity B had a Ge/ZnS coating, again optimized for $\lambda \in [5.5 \ldots 6.1]\,\mu$m. It was used for the muonic hydrogen measurements reported in Refs. [1, 2] and displayed the abovementioned light confinement time of 55 ns (Fig. 6).

- Cavity C was recently used in a follow-up experiment for the laser spectroscopy of muonic helium ions at a wavelength between 800 nm and 820 nm [8]. Here, a light confinement time of ~ 100 ns was routinely observed for pulse energies reaching 4 mJ.

In the next section we discuss the geometry of the multipass cavity as dictated by the experimental constraints. We then discuss the peculiarities of the light injection, present intensity distributions measured for various misalignments and compare them to simulations.

2. Geometry

The multipass cavity consists of two mirrors, each 190 mm long and 12 mm high, and separated by 25 mm, as shown in Figs. 1 and 2. The mirror length was limited to 190 mm by geometrical constraints in our setup even though the stop volume has a length of 200 mm. The illuminated volume was approximately 176 mm long. The thickness of the fused silica substrates was chosen to be 15 mm.

Mirror #1 (olive in Fig. 1) is assembled from a 170 mm long flat central piece and two 10 mm long cylindrical end pieces that ensure horizontal (along the muon beam axis) confinement of the light. The cylindrical end pieces were bolted to the flat center piece as detailed in Sec. 6.

According to simulations of the cavity (see Sec. 5.1), the radius of curvature of the cylindrical end pieces, R_{end}, has to be twice or four times the mirror spacing to ensure efficient light confinement. We chose a mirror spacing of 25 mm and hence an end piece radius of curvature of $R_{\mathrm{end}} = 100$ mm.

#206146 - $15.00 USD Received 11 Feb 2014; revised 22 Apr 2014; accepted 23 Apr 2014; published 22 May 2014

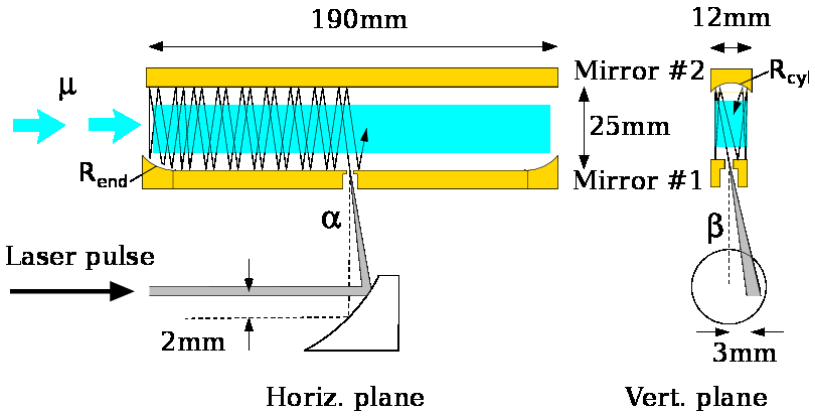

Fig. 2. Sketch of the cavity, indicating the light incoupling via the off-axis parabolic mirror (OAP). The blue shaded region indicates the muon stop volume to be illuminated by the light. The light is injected at an angle (horizontal α=40 mrad, vertical β=65 mrad) by a (parallel) displacement of the incoming light by 2 and 3.3 mm, respectively. The OAP has an off-axis focal length of 50.8 mm.

Mirror #2 (blue in Fig. 1) is a cylindrical mirror (cylinder axis along the muon beam axis) that ensures the vertical confinement of the light. Its radius of curvature $R_{\rm cyl}$ must *not* be twice or four times the mirror distance to avoid the laser beam retracing itself after a few round trips. This would result in a regular laser spot pattern instead of a washed-out homogeneous intensity distribution. We chose $R_{\rm cyl} = 110$ mm.

3. Light injection

Light is coupled into the multipass cavity through a hole in the middle of the flat piece of mirror #1. The hole has a diameter of only 0.63 mm at the optical surface of the mirror, and increases to 6 mm diameter on the back side of the mirror. Instead of a conical hole, we chose to drill three concentric holes (0.63 mm $\times$ 1 mm length, 3 mm diameter $\times$ 4 mm, and 6 mm diameter $\times$ 10 mm). The 0.63 mm diameter hole was drilled using ultrasonic drilling [9].

The laser light is focused into the center of the 1 mm long smallest part (0.63 mm diameter) of the injection hole, with a waist of 100 μm. For the geometry presented here, a lens with a focal length of f=50.8 mm could be used for our laser beam that has a wavelength of 6 μm and a 1 mm waist. We, however, chose to use a 90° off-axis parabolic mirror (OAP), due to geometric constraints inside the bore hole of our superconducting magnet.

The focusing element (lens or OAP) is used to control the size of the illuminated volume inside the cavity, as shown in Fig. 2: A parallel displacement of the incoming laser beam causes the light to enter the cavity at an angle (α, β in Fig. 2) with respect to the optical axis. A vertical displacement of 3.3 mm with respect to the OAP center results in a vertical injection angle of β=65 mrad and consequently a vertical size of the illuminated volume of 7 mm. Note that the cylindrical mirror #2 ensures that the light remains confined up to a maximum injection angle of 90 mrad.

Similarly, a horizontal laser light displacement of 2 mm on the OAP results in a horizontal injection angle of α=40 mrad. The cylindrical end pieces of mirror #1 ensure horizontal confinement of the light and a length of the illuminated volume of 176 mm.

A convenient side effect of the OAP focusing is that small beam pointing instabilities of our laser, which is $\sim$ 20 m away from the OAP, will only result in parallel displacements of the

#206146 - $15.00 USD Received 11 Feb 2014; revised 22 Apr 2014; accepted 23 Apr 2014; published 22 May 2014

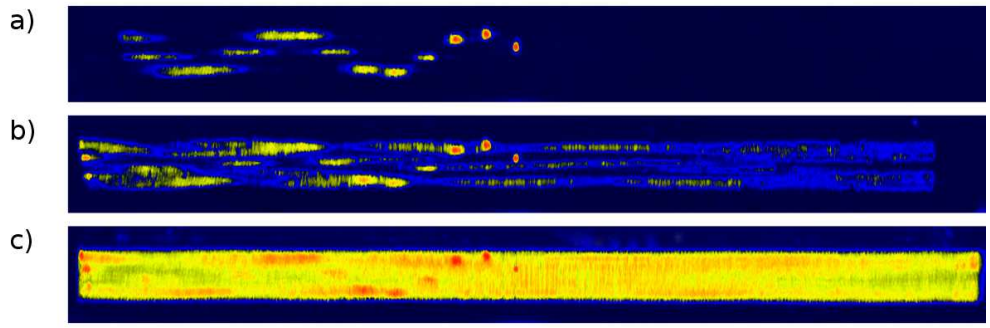

Fig. 3. Three intensity distributions measured in the cavity midplane (see Fig. 1). The distribution is measured at 850 nm in Cavity A using reflections from a thin moving wire inside the cavity (see Sec. 5.2 for details). Injected light started towards the top left. a: An absorber was placed in the left part of the cavity making the first quarter of the light roundtrip visible. b: The absorber was moved to the right end of the cavity. 3/4 of a round trip is seen. c: No absorber. The light fills the cavity volume.

laser beam on the OAP. The OAP will still ensure that all light will enter the cavity through the injection hole. Only the height of the illuminated volume may be slightly affected by laser beam pointing instabilities.

Light leaving the cavity through the injection hole is efficiently collected by the OAP. Monitoring this light reveals the light storage time and hence the quality of the light confinement inside the cavity. If the injection angle is chosen too small ($\alpha, \beta \approx 0$), most of the light escapes after one reflection. Efficient confinement is ensured only for α, β larger than three 1/e angles of the light focused into the injection hole.

4. Intensity distribution

We proceed now explaining how the light fills the cavity. We show simulations performed using simple ray optics as detailed in Sec. 5.1, and measurements using light reflected from a 25 μm thin wire that is moved through the center of the cavity, as explained in Sec. 5.2.

4.1. The first roundtrips

Figure 3 illustrates the working principle of the cavity. Shown are three measurements of the intensity pattern in the cavity midplane (Fig. 1).

Light injected at angles α, β (see Fig. 2) travels first to the left. The cylindrical mirror #2 ensures vertical confinement of the light. This gives rise to the vertical oscillation of the laser spot inside the cavity as it travels to the left. In Fig. 3(a) the light is intentionally absorbed before it reaches the cylindrical end piece of mirror #1. One can also observe how the initially focused beam spreads out in the horizontal direction.

In Fig. 3(b) the absorber was placed on the right hand side of the cavity. The left cylindrical end piece of mirror #1 causes the light to "turn around" and travel all the way to the right end of the cavity.

Figure 3(c) shows the intensity distribution measured inside the cavity without any absorber present. The volume is filled homogeneously. The rather low reflectivity of the mirrors used in this measurement prevents an even more homogeneous intensity distribution. In addition, the measurement procedure is at least partially responsible for the hot spots of the first few reflections. The light hits the wire used for measuring the distribution directly after entering the

#206146 - $15.00 USD Received 11 Feb 2014; revised 22 Apr 2014; accepted 23 Apr 2014; published 22 May 2014

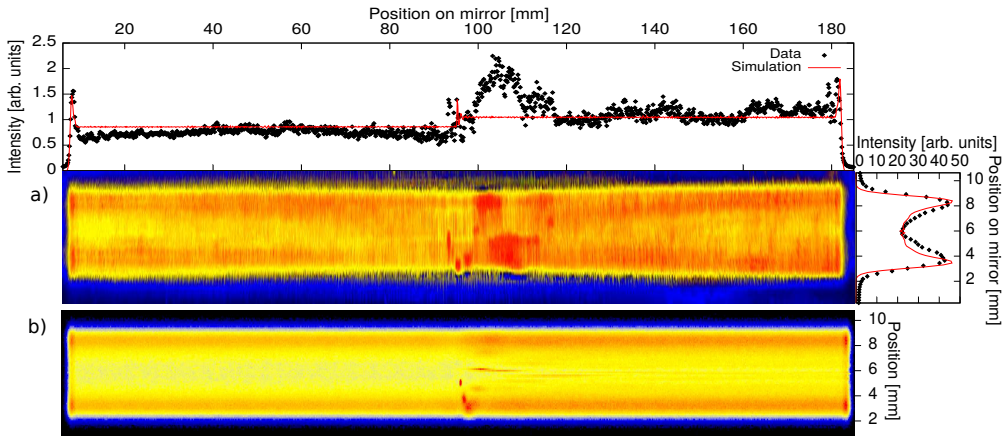

Fig. 4. The optimal distribution of light inside the cavity (a), compared to simulations (b, more details in Sec. 5.1)). Top: Intensity along the long axis. The spike in the red curve at z=95 mm indicates the location of the entrance hole. Right: Intensity along the vertical axis. For details see Sec. 4.2. Light injection is towards the bottom right.

cavity. Part of the light is scattered out of the cavity and is no longer available for filling the space above and below the hot spot after one or more round trips in the cavity.

4.2. Homogeneously filled cavity

Figure 4 shows the intensity distribution measured in the mid plane (see Fig. 1) of a well-aligned cavity. Also shown are projections of the intensity in the horizontal and vertical direction, together with simulations (see Sec. 5.1). The agreement is rather good, except for the region just right of the injection hole, where the data is well above the simulation. This is, however, believed to be an artifact of the measurement process as explained in Sec. 5.2.

Several features are visible in the projections. The step at the center of the horizontal distribution originates from the horizontal injection angle α (see Fig. 2): The light will first travel to the right, and several loss mechanisms reduce the intensity before the light arrives in the left part of the cavity: finite mirror reflectivity, possible imperfections at the transition from the flat to the cylindrical end piece of mirror #1, and the losses at the injection hole after half a roundtrip.

The higher intensity at both ends of the horizontal distribution can be understood in a ray optics picture: A ray arriving at the cylindrical end piece with an angle α will gradually reduce its angle in the cylindrical region until it eventually "turns around". This however results in an increased intensity, as the ray undergoes more reflections (per mm) at the turning point.

The same effect leads to the double-peak structure observed in the vertical intensity distribution: A ray initially traveling downwards at an angle β will gradually reduce its angle, perform more reflections per unit distance close to the lower turning point, but quickly traverse the central part of the mirror. This has the beneficial side-effect that the losses through the injection hole are smaller than expected from the average fluence inside the illuminated volume.

4.3. Mirror misalignments

Robustness against mirror misalignments was one of the design goals of the cavity. In our experiment [1, 2] we aligned the cavity mirrors and the injection optics (OAP) by measuring the storage time of the light (6μm wavelength) inside the cavity. The alignment procedure consists of aligning the mirrors by eye and final optimization of the storage time by tilting the

#206146 - $15.00 USD Received 11 Feb 2014; revised 22 Apr 2014; accepted 23 Apr 2014; published 22 May 2014

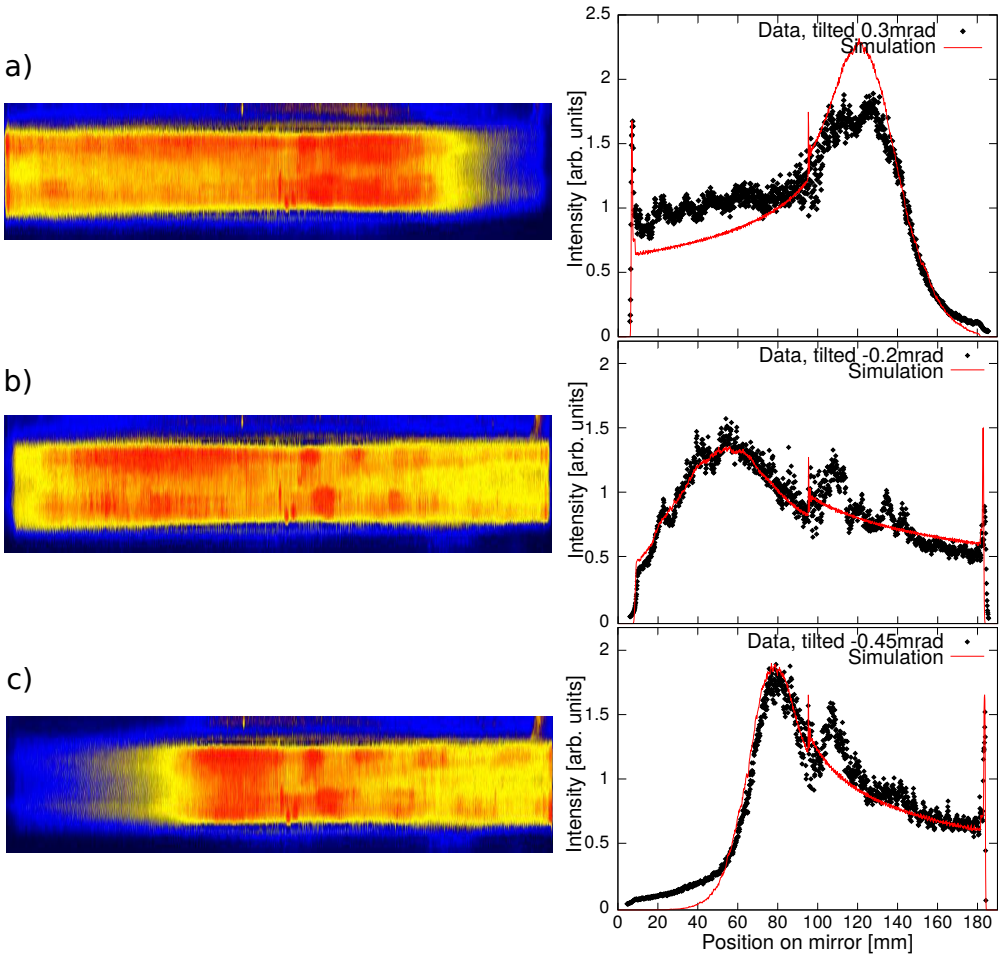

Fig. 5. Light distribution inside the cavity for different misalignments of mirror #1 around the vertical axis. The right images show the mean intensity of the left images in horizontal direction. Such a strong misalignment has never been observed in the experiment. However, the light is still confined in the cavity, even though mostly on one side.

mirrors. The first alignment does not have to be very accurate since the light with a wide range of angles is confined between the mirrors.

We closed and evacuated the setup and switched on a high magnetic field of 5 T. No remote-controlled or active mirror stabilization was employed. Still, no mirror misalignment was observed over the course of a few weeks.

This robustness originates from the small curvature radii of the employed cylinders: The 10 mm long cylindrical end pieces of mirror #1 with $R_{\mathrm{end}} = 100$ mm can capture light up to (horizontal) angles α of roughly 160 mrad. This corresponds to maximally allowed mirror misalignments of about ± 3 mrad (around the vertical axis), as the rays accumulate twice the mirror misalignment on each reflection of the misaligned mirror. For such enormous misalignments the light will only illuminate half of the enclosed volume, though.

Measurements of very misaligned cavity mirrors can be found in Fig. 5, together with simulations that describe the data quite well. Here, we tilted one of the mirrors by up to 0.45 mrad, corresponding to 85 μm displacement over the mirror length of 190 mm. Still, three quarters of

#206146 - $15.00 USD Received 11 Feb 2014; revised 22 Apr 2014; accepted 23 Apr 2014; published 22 May 2014

the cavity volume are filled with light, and no light is lost.

Vertical misalignments, i.e. rotation around the long axes of the mirrors, are much less critical. Such a mirror tilt is equivalent to a vertical displacement of the cylindrical mirror #2. The effect is hence only a vertical displacement of the illuminated volume. The strongly focusing cylindrical mirror ensures light confinement for vertical mirror tilts up to 10 mrad in the geometry presented here.

5. Simulation and measurement

5.1. Simulation

The intensity distribution was simulated using a simple ray-optics simulation. The simulation included the full geometry, including the possibility of misaligned mirrors.

It turns out that, for the curvature radii presented here, it is not necessary to take into account the exact reflection point in 3 dimensions between a ray and the curved and possibly tilted mirror surfaces. The cavity presented here could as well have been simulated by calculating the intersection of rays with flat mirrors and taking the curvature into account only for the reflection angle. Also, a simulation of Gaussian beams in the vertical dimension, propagated using ABCD-matrices, did not produce very different results.

The simulation used about 10^4 rays. Their initial position and angle in the injection hole were distributed according to the assumed Gaussian TEM_{00} mode of the injected laser beam. A simulation takes about a minute on a typical contemporary PC.

The simulation created the intensity profile on various planes parallel to the mirrors, as well as the time spectrum of the light leaving the cavity through the injection hole. This light was also used in the experiment to monitor adequate light confinement.

Interference effects are not expected to be important. The injected light is strongly focused, giving a large variety of ray angles. After a few roundtrips, every point receives light from many different directions.

5.2. Measurement of the intensity distribution in the cavity midplane

Cavity A was used for measuring the light distribution between the mirrors. A laser diode emitting light at 850 nm was used for these measurements. Although the reflective coating is optimized for a wavelength of 6μm, it has a sufficiently high reflectivity of more than 99.9% around 850 nm. Simulations showed that the distribution inside the cavity can be well estimated using ray optics with only minor influence of the laser wavelength.

The intensity distribution inside the cavity is measured by recording the light scattered from a thin wire (25μm diameter) which is moved along the long axis of the cavity mirrors. A video of the wire moving at constant velocity is recorded. The video is then converted into a single image by taking the maximum value recorded per pixel.

In general, the 25μm diameter of the wire is small enough to not severeley affect the light confinement. As mentioned above, we don't expect intensity variations on very small length scales, as interference is not expected to play a relevant role.

The finite diameter of the wire does however have an influence on measurement of the light distribution, causing artifacts like an overestimated intensity of the injected light and an apparent constriction of the illuminated volume next to the injection hole (see Fig. 4). Here, the injected light is still well collimated, and the wire can scatter a large fraction of the light.

5.3. Online monitoring of the intensity distribution

Cavity C used to measure several transition frequencies in muonic helium ions [8] at wavelengths $\lambda \in [800 \ldots 960]$ nm. Here, photo diodes (PD) have been used for online monitoring

#206146 - $15.00 USD Received 11 Feb 2014; revised 22 Apr 2014; accepted 23 Apr 2014; published 22 May 2014

of the intensity distribution. Each PD is connected to a ~ 10 mm long optical multi-mode fiber with a core diameter of a few hundred μm. Six of these PD-fiber-assemblies have been mounted in the support of the cylindrical mirror #2, and detect the light transmitted through the HR coating.

Four fibers are mounted close to the corners of the desired light distribution (i.e. at y=$\pm$3.5 mm in height, and z=$\pm$80 mm along the beam axis). The intensity distribution can be easily optimized by equalizing and maximizing the signal on all 4 PDs simultaneously. This enables us to optimize both the cavity mirror tilts and the light injection angle within a few minutes.

Two additional PD-fiber-assemblies monitor the light on the axis of the cavity (i.e at height y=0) where most of the atoms are.

The multi-mode fiber is used to limit both the light intensity experienced by the PDs and the field-of-view of each detector, thereby increasing the sensitivity to misalignments.

5.4. Fluence estimate and light decay time

The full simulation agrees very well with the measured intensity distribution and the lifetime of the light escaping through the injection hole.

However, already a simple estimate gives the average laser fluence achieved by the mirror setup: The laser light at $\lambda = 6\,\mu$m illuminates a region with an area of $176 \times 7\,\text{mm}^2$.

The losses are as follows: The mirror reflectivity or $R = 99.89\,\%$ results in $L_{\text{refl}} = 11 \times 10^{-4}$ per reflection. The injection hole with a diameter of 0.63 mm creates losses of $L_{\text{hole}} \approx 2/3 \times \pi/4 \times (0.63\,\text{mm})^2/(7 \times 176\text{mm}^2) = 1.7 \times 10^{-4}$ every *second* reflection (i.e. for each reflection on mirror #1). The additional factor of $\sim 2/3$ arises from the reduced laser fluence at the entrance hole location (cavity axis), see Fig. 4 and Sec. 4.2.

The two gaps of $\sim 50\,\mu$m width between the flat and the cylindrical parts of mirror #1 result in losses of $L_{\text{gap}} = (2 \times 0.05\,\text{mm})/176\,\text{mm} = 5.7 \times 10^{-4}$ every other reflection.

Hence, the total losses *per reflection* are $L_{\text{tot}} = L_{\text{refl}} + \frac{1}{2}L_{\text{hole}} + \frac{1}{2}L_{\text{gaps}} = 15 \times 10^{-4}$. This results in an average of $1/(15 \times 10^{-4}) = 670$ reflections.

With a mirror spacing of 25 mm (12 reflections per nanosecond) this should result in a light confinement lifetime of $\tau_{\text{conf}} \approx 56$ ns, in good agreement with the value measured in Cavity B at $\lambda = 6\,\mu$m (Fig. 6).

The pulse energy entering the cavity is 0.15 mJ. The resulting average fluence in the illuminated volume with a cross section of $A_{\text{illumi}} = 176 \times 7\,\text{mm}^2 = 12.3\,\text{cm}^2$ is therefore $F = 0.15\,\text{mJ} \cdot 670/12.3\,\text{cm}^2 = 8.0\,\text{mJ/cm}^2$.

This corresponds to half the saturation fluence of the $2S_{1/2}(F=1) \rightarrow 2S_{3/2}(F=2)$ transition in muonic hydrogen of 16.5 mJ/cm^2 [10]. The measurements [1, 2] confirm this estimate.

6. Technical considerations

6.1. Mirror #1

The substrates were manufactured by Lens-Optics[11]. Mirror #1 was assembled in our lab. For insensitivity against the 5 T magnetic field we used an aluminum bolt, a copper-beryllium washer and a titanium screw (see Fig. 7 for details). A microscope was used to adjust the optical surfaces of the flat and cylindrical parts. Great care must be taken to avoid rotational misalignment of the small cylinders with respect to the flat piece. A laser pointer beam was moved across the gap and the reflected beam was observed a few meters away. We achieved an accuracy of about 1 mrad in the ideal case. Such a precision is mandatory because a misalignment will lead to losses of the confined light: Light will experience a nonadiabatic vertical "kick" on the rotated cylinder which leads to a gradual increase in the illuminated height. Eventually,

#206146 - $15.00 USD Received 11 Feb 2014; revised 22 Apr 2014; accepted 23 Apr 2014; published 22 May 2014

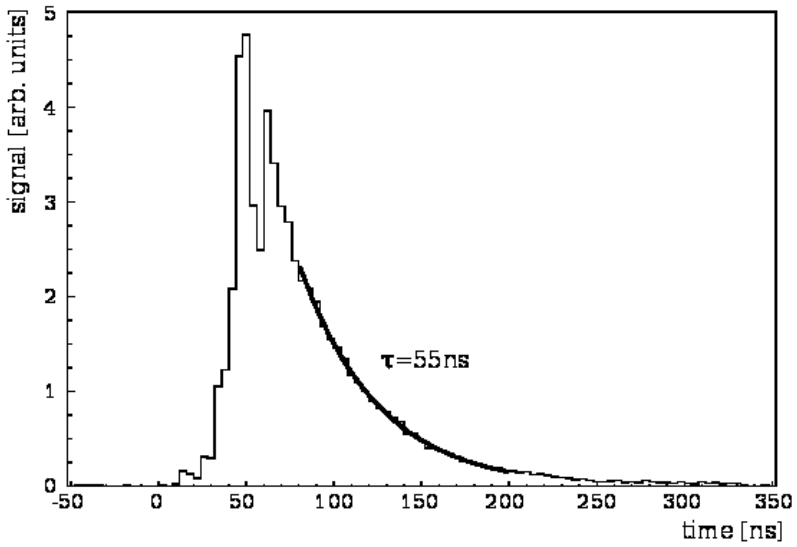

Fig. 6. Measured time spectrum of the 6 μm light leaving the cavity through the injection hole, recorded 2.5 m away from the mirror Cavity B. The structure of the 5 ns long pulse is visible after 1/2 and one round trip (peaks at very early times). After 1.5 round trips the light fills the whole cavity and decays with a lifetime $\tau_{\text{conf}} = 55$ ns (see Sec. 5.4).

light will spill over the upper and lower edges of the cavity mirrors. Additionally, a horizontal non-adiabatic kick will be introduced, when the cylinder of the end piece does not end tangentially with the plain of the main substrate. Care must be taken during fabrication and when choosing the end piece.

After aligning the small cylinders with high precision we glued small glass pieces onto the back side of the mirror, either using Torr Seal [12] or EpoTek 353ND [13]. Both display low outgassing, but the latter can stand higher temperatures during the coating process.

6.2. Mirror #2

Mirror #2 is a simple cylinder. Care must be taken to avoid a toroidal shape of mirror #2. Such a torus can easily occur in the manufacturing process of the long cylindrical mirror. Simulations show that the radius of curvature along the cylinder axis should be well above 100 m. Otherwise the light will be confined to a small central part of the cavity.

6.3. Coating

The dielectric ZnS/Ge coating [14] of Cavity B provided a high reflectivity of $R = 99.89\,\%$ over a wavelength range of $\lambda = 5.5 \ldots 6.1\,\mu$m. This was measured using pulsed laser cavity ringdown in a 50 cm long flat-concave cavity built from 1" witness samples. An even higher reflectivity ($R = 99.97\,\%$ or better) had previously been achieved for Cavity A by a ThF_4/ZnSe coating [15], but the small amount of alpha particles emitted from the coating could not be tolerated in our setup. Cavity C was recently used at $\lambda \approx 810$ nm. The coating [16] has a reflectivity of 99.97 % for $\lambda \in [800 \ldots 975]$ nm needed for the muonic helium measurements [8].

#206146 - $15.00 USD Received 11 Feb 2014; revised 22 Apr 2014; accepted 23 Apr 2014; published 22 May 2014

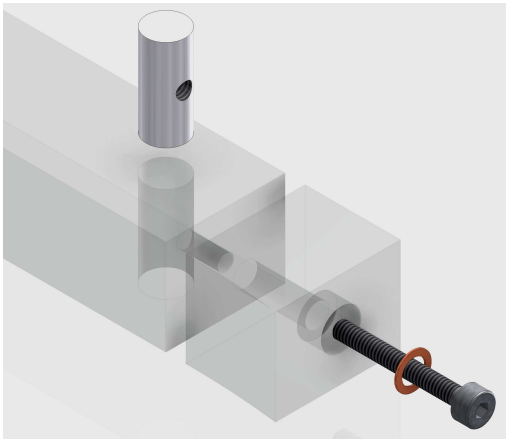

Fig. 7. Detail drawing of a cylindrical end piece and the parts used for mounting it. An aluminum bolt, a copper-beryllium washer and a titanium screw are used for fixing the substrate in its final position. Compatibility with vacuum, high temperature during coating, and a strong magnetic field were reasons for choosing these materials.

7. Conclusions

A multipass mirror cavity has been presented that allows illumination of a very large and very elongated volume. Such a volume can not easily be illuminated by other mirror configurations, as large cavity waists result in excessive sensitivity to mirror misalignment. Our cavity achieves an intensity distribution which is homogeneous within $\pm 30\,\%$, and is very robust against misalignments. No active mirror stabilization is required.

In the measurement of the Lamb shift in muonic hydrogen [1, 2] and muonic helium ions [8] such cavities have been successfully used to illuminate a volume of $176 \times 25 \times 7\,\mathrm{mm}^3$ at wavelengths $\lambda \in [5.5 \ldots 6.1]\,\mu\mathrm{m}$ and $\lambda \in [800 \ldots 820]\,\mathrm{nm}$, respectively. Larger volumes can be easily realized.

Such a cavity may be useful for a variety of other experiments. Optical excitation of a beam of hydrogen atoms to the metastable 2S state for a precision measurement of the Rydberg constant [17] can circumvent the systematic uncertainties that originate from electron bombardment [18].

Another application may be transverse cooling of a beam of atoms or molecules. Using two such cavities, 2D transverse cooling may be achieved. This may for example prove useful for experiments with antihydrogen $\overline{\mathrm{H}}$ beams for spectroscopy [19] or the measurement of the free fall of $\overline{\mathrm{H}}$ atoms [20, 21, 22].

The cavity may also be used to create a "light curtain" illuminating a region of e.g. $20\,\mathrm{cm} \times 10\,\mathrm{cm}$, over a distance of a cm or more along the beam axis [23], as sketched in Fig. 8. Laser spectroscopy of Muonium (μ^+e^-) [24, 25] or Positronium (Ps $\equiv e^+e^-$) [26], or creation of Rydberg Ps [27], where exotic atoms are emitted from a surface and into a large solid angle, could benefit from such a geometry. Also, optical excitation of H atoms created in neutron decay [28] requires transverse illumination of a large volume inside a neutron guide.

Acknowledgments

The authors would like to thank K. Linner, W. Simon, and the excellent workshops of MPQ and PSI for the support in designing and building the various mechanics, and H. Brückner of MPQ for help on electronics. We thank S. Spielmann-Jäggi and L. Carroll of PSI for measuring

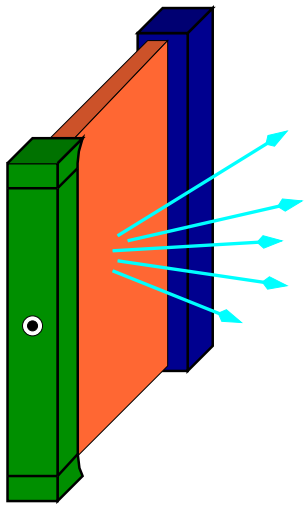

Fig. 8. A slightly different geometry of the cavity presented here may be used to create a "light curtain", for example $20 \times 10 \times 1\,\mathrm{cm}^3$ (red) [23]. This can be useful in a variety of experiments, e.g. with large or very divergent particle beams (light blue arrows) [24, 25, 26, 27, 28] (see text).

substrate and mirror properties. The people at Lens Optics GmbH, dama technologies ag, Lohnstar Optics Inc., Umicore Coating Services Ltd., and Advanced Thin Films have done a great job. M.D., J.G., J.K., T.N., and R.P. acknowledge support from the European Research Council under StG. 279765, A.A. and K.S. from SNF 200021L_138175, and T.W.H. from the Max-Planck-Society and the Max-Planck-Foundation.

J.V.'s present address is: Institut für Physik, Carl von Ossietzky Universität, 26129 Oldenburg, Germany. T.W.H. is also at: Ludwig-Maximilians-Universität, 80539 Munich, Germany.

#206146 - $15.00 USD Received 11 Feb 2014; revised 22 Apr 2014; accepted 23 Apr 2014; published 22 May 2014